

Communication

Anisotropic Assembly of Ag52 and Ag76 Nanoclusters

Jia-Wei Liu, Lei Feng, Haifeng Su, Zhi Wang, Quan-Qin Zhao,
Xingpo Wang, Chen-Ho Tung, Di Sun, and Lan-Sun Zheng

J. Am. Chem. Soc., **Just Accepted Manuscript** • DOI: 10.1021/jacs.7b12777 • Publication Date (Web): 18 Jan 2018

Downloaded from <http://pubs.acs.org> on January 18, 2018

Just Accepted

“Just Accepted” manuscripts have been peer-reviewed and accepted for publication. They are posted online prior to technical editing, formatting for publication and author proofing. The American Chemical Society provides “Just Accepted” as a free service to the research community to expedite the dissemination of scientific material as soon as possible after acceptance. “Just Accepted” manuscripts appear in full in PDF format accompanied by an HTML abstract. “Just Accepted” manuscripts have been fully peer reviewed, but should not be considered the official version of record. They are accessible to all readers and citable by the Digital Object Identifier (DOI®). “Just Accepted” is an optional service offered to authors. Therefore, the “Just Accepted” Web site may not include all articles that will be published in the journal. After a manuscript is technically edited and formatted, it will be removed from the “Just Accepted” Web site and published as an ASAP article. Note that technical editing may introduce minor changes to the manuscript text and/or graphics which could affect content, and all legal disclaimers and ethical guidelines that apply to the journal pertain. ACS cannot be held responsible for errors or consequences arising from the use of information contained in these “Just Accepted” manuscripts.

Anisotropic Assembly of Ag₅₂ and Ag₇₆ Nanoclusters

Jia-Wei Liu,[†] Lei Feng,[†] Hai-Feng Su,[‡] Zhi Wang,[†] Quan-Qin Zhao,[†] Xing-Po Wang,[†] Chen-Ho Tung,[†] Di Sun^{*,†,‡} and Lan-Sun Zheng[‡]

[†]Key Lab of Colloid and Interface Chemistry, Ministry of Education, School of Chemistry and Chemical Engineering, Shandong University, Jinan, 250100, People's Republic of China.

[‡]State Key Laboratory for Physical Chemistry of Solid Surfaces and Department of Chemistry, College of Chemistry and Chemical Engineering, Xiamen University, Xiamen, 361005, People's Republic of China.

Supporting Information

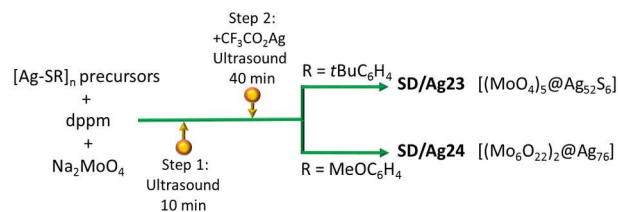
ABSTRACT: Although there has been an upsurge of interest in anisotropic assembly of inorganic nanoparticles, atomically precise self-assembly of anisotropic metal clusters is extremely rare. Herein, we presented two novel silver nanoclusters, Ag₅₂ (**SD/Ag23**) and Ag₇₆ (**SD/Ag24**), which are interiorly templated by five MoO₄²⁻ and a pair of Mo₆O₂₂⁸⁻ anions, respectively, and co-protected by bridging RSH and terminal diphosphine ligands exteriorly. Regiospecific distribution diphosphine ligands on the surface and the arrangement of multiple molybdate templates within the nanoclusters synergistically tailor their shapes to anisotropic oblate spheroid and elongated rod, respectively. This work not only open up new avenues for the synthesis of silver nanoclusters with novel metal skeleton shapes and anisotropic surface structures, but also give important insights for the anisotropic growth of silver nanoclusters through surface modifications or/and template organizations.

Due to the close structure-property correlations, anisotropic nanoparticles have exhibited fascinating size- and shape-dependent properties, thus pushing the anisotropic growth and assembly of nanoparticles to be an enthusiastically pursued area of exploration.¹ However, down-sizing of them to nanoclusters caused the anisotropic assembly rather difficult owing to the inherently more complex assembly environments and the difficulty to achieve the atomically precise structures, especially for high-nuclearity metal clusters.² Compared to ubiquitous isotropic spherical silver nanoclusters, anisotropic nanoclusters have regiospecific surface structures and metal skeleton shapes, thus defining regiospecific functionality sites such as catalysis active centers. Retrospecting the history of reported silver nanoclusters, we found most of them are spherical or quasi-spherical,³⁻¹¹ whereas only limited examples showed anisotropic geometries.¹² Based on the inspirations from the anisotropic nanoparticles, understanding the coordination preferences of different ligands is probably the key for controlling the orientation and spatial arrangement of them to achieve anisotropic shapes,¹³ however, such task is still hard to be realized at the molecular level. As one of the most powerful tools, single crystal X-ray diffraction (SCXRD) can give atomically precise metal and ligand spatial arrangement landscapes. Thus, it is imperative to access the crystallography of these anisotropic silver nanoclusters to elucidate the overarching factors and local mechanisms leading to anisotropic as-

sembly. For mixed-ligands co-capped silver nanoclusters, different ligands dissimilar in their steric hindrance and coordination preference play different roles in the assembly so as to build the anisotropic nanoclusters. To address above-mentioned challenges much more experimental evidences are needed, especially for the vivid single crystals structures of anisotropic silver nanoclusters.

With these considerations in mind, we isolated two novel silver nanoclusters using RSH (*t*BuC₆H₄SH for **SD/Ag23** and MeOC₆H₄SH for **SD/Ag24**) and dpmm (dpmm = Bis-(diphenylphosphino)methane) ligands (Scheme 1). Their formulae were confirmed as (HNEt₃)₁₀[(MoO₄)₅@Ag₅₂S₆(*t*BuC₆H₄S)₂₀(dpmm)₁₀(MoO₄)₁₀] (**SD/Ag23**) and [(Mo₆O₂₂)₂@Ag₇₆(MeOC₆H₄S)₂₈(dpmm)₈(MoO₄)₁₆(H₂O)₈·8CH₃OH·4CH₃CN] (**SD/Ag24**). Two silver nanoclusters have following features: (a) Their metal shells and ligands show typical anisotropic shapes and regiospecific distributions, respectively; (b) Both of them are formed by multiple molybdates (up to five MoO₄²⁻ in **SD/Ag23** and two Mo₆O₂₂⁸⁻ in **SD/Ag24**) templates; (c) Dppm as terminator ligates on the cyclic periphery of disc-like Ag₅₂ and two ends of rod-like Ag₇₆ nanoclusters.

Scheme 1. Synthetic Routes for **SD/Ag23** and **SD/Ag24**.



Details of the synthesis and some basic characterizations for them are shown in the Supporting Information (SI). The molecular structures of **SD/Ag23** and **SD/Ag24** were determined by SCXRD analysis (Table S1). They crystallize in monoclinic *C*2/*m* and tetragonal *I*-4 space groups, respectively. **SD/Ag23** is an anionic oblate nanocluster with a C_{2h} symmetry. The asymmetric unit of **SD/Ag23** contains a quarter of Ag₅₂ cluster. **SD/Ag23** is an oblate spheroid composed of 52 silver atoms, 10 dpmm, 20 *t*BuC₆H₄S⁻ ligands, 6 S²⁻ and 15 MoO₄²⁻ anions (Figure 1a and 1b). The equatorial and polar diameters of **SD/Ag23** is 2.9 and 1.8 nm, respectively, if removing the organic shell, they are 1.8 and 0.8 nm, respectively. The 52 Ag atoms can be divided into two categories: 2 Ag atoms (Ag1

and Ag1¹) in the inner of the cluster along the polar radius and 50 Ag atoms on the surface, which can be seen as a layer-by-layer motif with totally five layers (Figure 1c). Each layer from pole to equator to opposite pole contains 5, 10, 20, 10, 5 silver atoms, thus forming metallic 5-, 10- and 20-gons, analog to latitude lines on the oblate spheroid. The adjacent polygons are further linked by *t*BuC₆H₄S⁻ and MoO₄²⁻ anions as well as the argentophilic interactions¹⁴ in the range of 2.858(5)-3.370(2) Å. Alternatively, the skeleton of Ag₅₀ shell is composed of two pentagons at two poles with each rounded by five alternate squares and trigons, ten squares and ten boat-like hexagons near to equator region (Figure 1d), that is total 10 trigons, 20 squares, 2 pentagons, 10 hexagons.

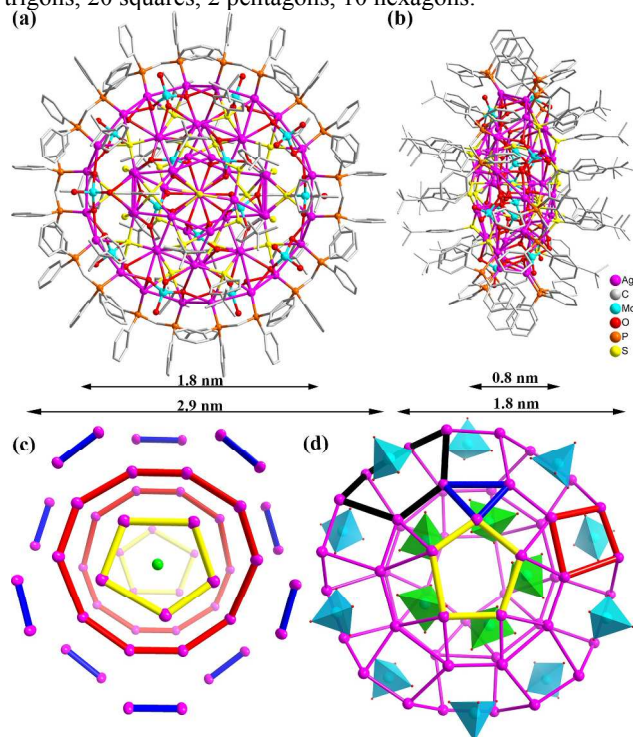


Figure 1. (a) and (b) The X-ray crystal structure of Ag₅₂ nanoclusters viewed along two orthogonal directions. (c) The layer-by-layer structure of 52-silver-skeleton. Different layers are highlighted individually by different colors. Two green balls along the polar radius direction are two interior Ag atoms. (d) The Ag₅₀ shell composed of diverse polygons. One boat-like hexagon, pentagon, tetragon and trigon were highlighted by bold black, yellow, red and blue bonds, respectively. Five interior and ten exterior MoO₄²⁻ anions are represented by green and cyan polyhedral.

All dppm ligands as μ_2 bridges seal the cyclic periphery of Ag₅₂ cluster (Ag-P distances: 2.374(6)-2.383(7) Å), whereas 20 *t*BuC₆H₄S⁻ ligands cover on the 20 Ag₄ squares of oblate spheroid up and down in a unified μ_4 mode (Ag-S distances: 2.268(9)-2.908(5) Å), which gives an anisotropic distributions for *t*BuC₆H₄S⁻ and dppm ligands. Totally 15 MoO₄²⁻ anions are found both inside and outside of Ag₅₂ cluster, of which five (green polyhedra in Figure 1d) in the cavity as anion templates adopt a unified $\mu_8\text{-}\eta^2\text{:}\eta^2\text{:}\eta^2\text{:}\eta^2$ mode to support the Ag₅₂ cluster (Figure S1) and the other ten (cyan polyhedra in Figure 1d) coordinate to the equator region in $\mu_7\text{-}\eta^2\text{:}\eta^3\text{:}\eta^2\text{:}\eta^0$, $\mu_5\text{-}\eta^2\text{:}\eta^3\text{:}\eta^0\text{:}\eta^0$, or $\mu_6\text{-}\eta^2\text{:}\eta^2\text{:}\eta^2\text{:}\eta^0$ mode where dppm ligands are alternately arranged with MoO₄²⁻. Two $\mu_3\text{-S}^{2-}$ ions (S7 and S7¹) sit on two poles of oblate spheroid and bind to two interior Ag atoms to form the central axis (S7-Ag1-Ag1¹-S7) along the polar radius direction (Figure S2), whereas the other four $\mu_2\text{-S}^{2-}$ locate in the inner of Ag₅₂ cluster near to the equatorial

plane (Figure S3, Ag-S distances: 2.669(6)-2.834(8) Å). These S²⁻ ions should be *in situ* generated from the C-S bond cleavage of *t*BuC₆H₄SH ligands as seen in similar assembly systems.^{7,14c} (symmetry code: $i = -x+1, -y+1, -z$)

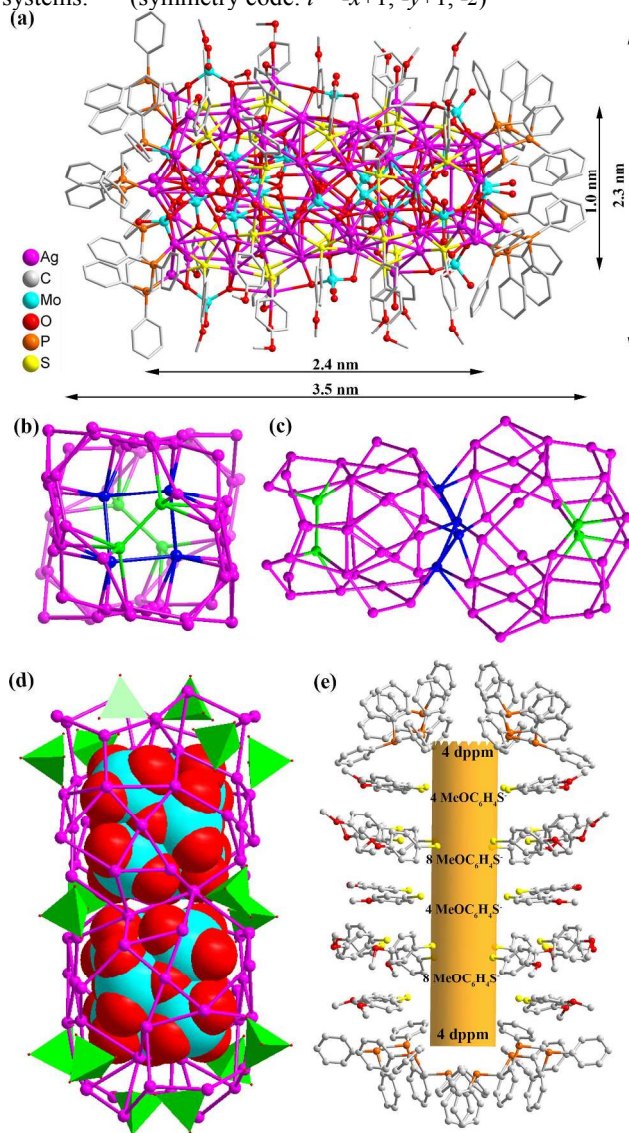


Figure 2. (a) The molecular structure of Ag₇₆ nanocluster. (b) and (c) Two orthogonal views of skeleton of Ag₇₆ nanocluster with inner four and shared four silver atoms highlighted by green and blue, respectively. (d) Two Mo₆O₂₈⁸⁻ templates caged in a Ag₇₆ nanocluster. The green tetrahedra are 16 MoO₄²⁻ anions on the surface. (e) Anisotropic distributions of dppm and MeOC₆H₄S⁻ ligands around the Ag₇₆ shell simplified to a yellow pillar.

More striking, not only the numbers of Ag atoms in each layer but also the numbers of dppm, *t*BuC₆H₄S⁻ ligands and MoO₄²⁻ ions are 5 or multiples of 5, which imposes a *quasi*-five-fold symmetry of the overall oblate spheroid (Figure S4). As we know, the odd orders of symmetry are disfavored,¹⁵ thus artificial molecular clusters with 5- even 7-fold symmetry were still rare,¹⁶ although such symmetries have been found in biomacromolecules.¹⁷

When changing the bulk *t*BuC₆H₄SH to MeOC₆H₄SH, a rod-like Ag₇₆ cluster was isolated. SCXRD analysis revealed that it sits on the crystallographic inversion center (*i*) that is passed by a crystallographic 4-fold axis (*C*₄), giving the Ag₇₆ nanocluster a *S*₄ symmetry. The asymmetric unit of **SD/Ag24** contains a quarter of Ag₇₆ cluster and one CH₃OH and CH₃CN

molecules. The **SD/Ag24** is a neutral nanocluster with a long rod geometry. As shown in Figure 2a, this 76-nucleus nanocluster is template by two $\text{Mo}_6\text{O}_{22}^{8-}$ anions in the interior and capped by 8 dppm, 28 $\text{MeOC}_6\text{H}_4\text{S}^-$, 16 MoO_4^{2-} , 8 aqua ligands on the surface. The diameter of square cross-section (Figure 2b) and length of **SD/Ag24** is 2.3 and 3.5 nm, respectively, if removing the organic shell, they are 1.0 and 2.4 nm, respectively.

Among 76 Ag atoms shown in Figure 2c, four locate in the nanocluster (green balls), thus the outer shell of **SD/Ag24** contains only 72 Ag atoms. The Ag_{76} cluster can be seen as two 40-nucleus cages mutually rotated by 90° then fused together by sharing four silver atoms (blue balls) at the waist section of the cluster. The $\text{Ag}\cdots\text{Ag}$ distances within the argentophilic interaction range are 2.8487(10)-3.3604(10) Å. Within the cluster, two *in situ* generated bicubane $\text{Mo}_6\text{O}_{22}^{8-}$ anions from Na_2MoO_4 act as templates to support the cluster through Ag-O interactions (Figure 2d). For each $\text{Mo}_6\text{O}_{22}^{8-}$ anion 26 silver atoms are coordinated to it with the Ag-O distances of 2.271(6)-2.563(6) Å (Figure S5). Notably, such bicubane $\text{Mo}_6\text{O}_{22}^{8-}$ anion has only been observed in a Ag_{58} mango-like nanoclusters,¹⁸ but only one was trapped. Sixteen MoO_4^{2-} anions were found on the surface of the Ag_{76} cluster, six ($\mu_7\text{-}\eta^2\text{-}\eta^3\text{-}\eta^2\text{-}\eta^0$, $\mu_8\text{-}\eta^3\text{-}\eta^3\text{-}\eta^2\text{-}\eta^0$, and $\mu_5\text{-}\eta^2\text{-}\eta^3\text{-}\eta^0\text{-}\eta^0$) on each end of the cluster and four ($\mu_6\text{-}\eta^2\text{-}\eta^3\text{-}\eta^0\text{-}\eta^0$) on the waist region. All $\text{MeOC}_6\text{H}_4\text{S}^-$ ligands are coordinated at the rod body region, forming a five layers distribution. Each $\text{MeOC}_6\text{H}_4\text{S}^-$ ligand caps on the irregular Ag_4 quadrangle with a unified μ_4 mode (Ag-S distances: 2.451(2)-2.730(2) Å). The numbers of $\text{MeOC}_6\text{H}_4\text{S}^-$ ligands in each layer from one end to another are 4, 8, 4, 8, 4. Eight dppm ligands are anchored on both ends of rod equally (Figure 2e). There are additional eight aqua ligands on the surface to finish the coordination geometry of silver atoms. To the best of our knowledge, this nanocluster is the largest silver nanocluster templated by molybdates.

Notably, both Ag_{52} and Ag_{76} nanoclusters clearly exhibit anisotropic shapes and ligands distributions, which should be caused by the synergetic effects from anion template and ligand category. The overall arrangement of multiple anions in the interior dominate the geometries of silver nanoclusters. On the other hand, the differences in coordination preferences and steric hindrances between RSH and dppm give them selectively covered on the specific regions, forming the regiospecific organic coatings. In details, the anisotropic shape of Ag_{52} nanocluster is benefited from the circular arrangement of multiple MoO_4^{2-} anion templates which dictates the cyclic profile of Ag_{52} nanocluster that is further shaped by the bulkier $t\text{BuC}_6\text{H}_4\text{S}^-$ ligand and terminator dppm ligands to form a discrete oblate spheroid, similar to a round fragment cut from a 2D layer. The linear arrangement of a pair of $\text{Mo}_6\text{O}_{22}^{8-}$ anion decides the final shape of Ag_{76} nanocluster to be a rod which is covered by five-layered $\text{MeOC}_6\text{H}_4\text{S}^-$ ligands on the body of rod and further polymerization is terminated by dppm at both ends. The longer diphosphines such as 1,4-bis(diphenylphosphino)butane (dppb) disfavor to the formation of such kind of anisotropic Ag clusters as compared to previously reported tetrahedral Ag_{24} clusters.¹⁹

The positive-ion ESI-MS of **SD/Ag23** dissolved in CH_2Cl_2 shows four dominated +3 signals (**1a-1d**, Figure 3). The most dominated peak at $m/z = 5184.17$ corresponds to $[(\text{HNEt}_3)_2(\text{MoO}_4)_5@(\text{Ag}_{52}\text{S}_6(t\text{BuC}_6\text{H}_4\text{S})_{20}(\text{dppm})_{12}(\text{MoO}_4)_8(\text{H}_2\text{O})_5(\text{CH}_2\text{Cl}_2)_7]^{3+}$ (**1d**, calcd. $m/z = 5184.08$), whereas species **1c** has the same core $[(\text{MoO}_4)_5@(\text{Ag}_{52}\text{S}_6)]$ but with different number of outer ligands compared with **1d** (exp. $m/z = 4914.66$;

calc. $m/z = 4914.70$), which indicated the core of **SD/Ag23** can keep integrity in CH_2Cl_2 . However, another two species with lower abundance, **1a** and **1b**, were also detected at lower m/z range, indicating the equilibrium between parent cluster and some fragments in solution. By matching the experimental and simulated isotope distributions, we ascribed two fragments to $[(\text{HNEt}_3)_2(\text{MoO}_4)_5@(\text{Ag}_{39}\text{S}_6(t\text{BuC}_6\text{H}_4\text{S})_{12}(\text{dppm})_8(\text{MoO}_4)_2(\text{H}_2\text{O})_3(\text{CH}_2\text{Cl}_2)_5]^{3+}$ (exp. $m/z = 3342.11$; calc. $m/z = 3342.19$) and $[(\text{HNEt}_3)_2(\text{MoO}_4)_5@(\text{Ag}_{40}\text{S}_6(t\text{BuC}_6\text{H}_4\text{S})_{13}(\text{dppm})_8(\text{MoO}_4)_2(\text{H}_2\text{O})_6(\text{CH}_2\text{Cl}_2)_2]^{3+}$ (exp. $m/z = 3384.15$; calc. $m/z = 3384.25$), respectively. The details of assigned formulae for **1a-1d** were listed in Table S3. We also checked the mother solution after reaction by ESI-MS (Figure S11) to explore the possible intermediates to the final Ag_{52} cluster in the solid state. The positive-ion ESI-MS showed only two species (**1a'** and **1b'**) in the $m/z = 2000$ -3000 range and both are much smaller fragments with core compositions of $[(\text{MoO}_4)_5@(\text{Ag}_{23}\text{S}_2)]$ and $[(\text{MoO}_4)_5@(\text{Ag}_{24}\text{S}_2)]$, respectively (Table S4), which suggests that the formation of **SD/Ag23** may follow a core-expansion route from the inside out around five inner MoO_4^{2-} templates.

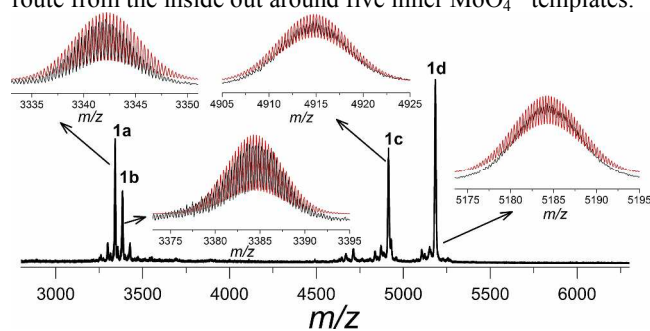


Figure 3. (a) Positive-ion ESI-MS of **SD/Ag23** dissolved in dichloromethane. Insets show the experimental (black line) and the simulated (red line) isotopic distribution patterns of **1a-1d**.

For **SD/Ag23**, an emission peak was observed in NIR region at ca. 775 nm ($\lambda_{\text{ex}} = 365$ nm, Figure 4). The red light emission of **SD/Ag23** should be assigned to a ligand-to-metal-charge-transfer (LMCT, $\text{S } 3p \rightarrow \text{Ag } 5s$) transition mixed with cluster-centered transitions.²⁰ When cooling to lower temperature, the maximum emission wavelength has barely change, but the emission intensity gradually increases.

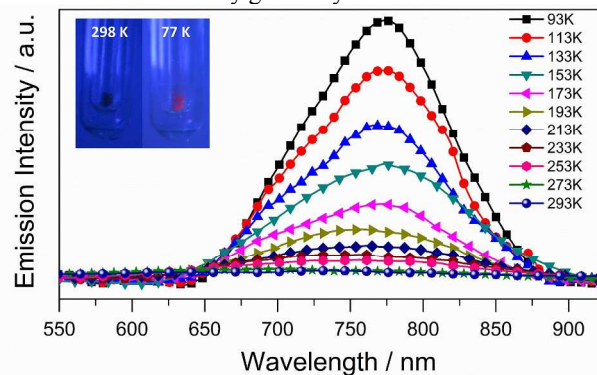


Figure 4. The emission spectra of **SD/Ag23** recorded from 93 to 293 K. Insets show the photographs of sample **SD/Ag23** under a hand-held UV lamp (365 nm) at 298 and 77K.

In conclusion, we synthesized and characterized two unprecedented mixed ligands co-protected Ag_{52} and Ag_{76} nanoclusters that are interiorly templated by five MoO_4^{2-} and a pair of bicubane $\text{Mo}_6\text{O}_{22}^{8-}$ anions, respectively. Regiospecific distribution of diphosphine ligands on the surface and the ar-

1 rangement of multiple molybdate templates within the
2 nanoclusters synergetically tailor their shapes to anisotropic
3 oblate spheroid and elongated rod, respectively. This work not
4 only rich the anisotropic silver clusters but also give important
5 insights for the anisotropic growth of silver nanoclusters
6 through surface modifications or/and template organizations.

7 ASSOCIATED CONTENT

8 **Supporting Information.** Experimental details, detailed crystal-
9 lographic structure and data including the CIF file, PXRD, IR,
10 UV-Vis, EDS mapping and ESI-MS. This information is available
11 free of charge via the internet at <http://pubs.acs.org>.

12 AUTHOR INFORMATION

13 Corresponding Author

14 dsun@sdu.edu.cn

16 ACKNOWLEDGMENT

17 This work was supported by the NSFC (Grant No. 21571115), the
18 Natural Science Foundation of Shandong Province (Nos.
19 ZR2014BM027 and ZR2017MB061), Young Scholars Program of
20 Shandong University (2015WLJH24), and the Fundamental Re-
21 search Funds of Shandong University (104.205.2.5 and
22 2015JC045). We thank Prof. Shu-Ao Wang and Dr. Wei Liu in
23 Soochow University for luminescence spectra measurements.

24 REFERENCES

- 25 1. (a) Jin, R. C.; Cao, Y. C.; Hao, E. C.; Metraux, G. S.; Schatz, G. C.;
26 Mirkin, C. A. *Nature* **2003**, *425*, 487–490. (b) Gan, L.; Cui, C.;
27 Heggen, M.; Dionigi, F.; Rudi, S.; Strasser, P. *Science* **2014**, *346*,
28 1502–1506. (c) Kim, F.; Song, J. H.; Yang, P. D. *J Am Chem Soc*
29 *2002*, *124*, 14316.
- 30 2. (a) Corrigan, J. F.; Fuhr, O.; Fenske, D. *Adv Mater* **2009**, *21*,
31 1867–1871. (b) Jin, R.; Zeng, C.; Zhou, M.; Chen, Y. *Chem Rev*
32 **2016**, *116*, 10346–10413.
- 33 3. (a) Wang, Z.; Su, H.-F.; Tan, Y.-Z.; Schein, S.; Lin, S.-C.; Liu, W.;
34 Wang, S.-A.; Wang, W.-G.; Tung, C.-H.; Sun, D.; Zheng, L.-S.
35 *Proc. Natl. Acad. Sci. USA* *2017*, *114*, 12132–12137. (b) Rais, D.;
36 Yau, J.; Mingos, D. M. P.; Vilar, R.; White, A. J. P.; Williams, D. J.
37 *Angew. Chem., Int. Ed.* **2001**, *40*, 3464–3467.
- 38 4. Bian, S.-D.; Jia, J.-H.; Wang, Q.-M. *J. Am. Chem. Soc.* **2009**, *131*,
39 3422–3423.
- 40 5. Dhayal, R. S.; Liao, J.-H.; Liu, Y.-C.; Chiang, M.-H.; Kahlal, S.;
41 Saillard, J.-Y.; Liu, C. W. *Angew Chem Int Ed* **2015**, *54*, 3702–3706.
- 42 6. Ahmar, S.; MacDonald, D. G.; Vijayaratnam, N.; Battista, T. L.;
43 Workentin, M. S.; Corrigan, J. F. *Angew Chem Int Ed* **2010**, *49*,
44 4422–4424.
- 45 7. Li, G.; Lei, Z.; Wang, Q.-M. *J. Am. Chem. Soc.* *2010*, *132*, 17678–
46 17679
- 47 8. Fenske, D.; Persau, C.; Dehnen, S.; Anson, C. E. *Angew Chem Int*
48 *Ed* **2004**, *43*, 305–309.
- 49 9. Liu, Y. Y.; Najafabadi, B. K.; Fard, M. A.; Corrigan, J. F. *Angew*
50 *Chem Int Ed* **2015**, *54*, 4832–4835.
- 51 10. Chen, Z. Y.; Tam, D. Y. S.; Mak, T. C. W. *Chem Commun* **2016**, *52*,
52 6119–6122.
- 53 11. Anson, C.; Eichhoefer, A.; Issac, I.; Fenske, D.; Fuhr, O.; Sevillano,
54 P.; Persau, C.; Stalke, D.; Zhang, J. *Angew Chem Int Ed* **2008**, *47*,
55 1326–1331.
- 56 12. (a) Liu, X.; Yang, H.; Zheng, N.; Zheng, L. *Eur J Inorg Chem* **2010**,
57 2084–2087. (b) Huang, R.-W.; Xu, Q.-Q.; Lu, H.-L.; Guo, X.-K.;
58 Zang, S.-Q.; Gao, G.-G.; Tang, M.-S.; Mak, T. C. W. *Nanoscale*
59 **2015**, *7*, 7151–7154.
- 60 13. Lohse, S. E.; Burrows, N. D.; Scarabelli, L.; Liz-Marzan, L. M.;
Murphy, C. J. *Chem Mater* **2014**, *26*, 34–43.
- (a) Schmidbaur, H.; Schier, A. *Angew Chem Int Ed* **2015**, *54*, 746–
784. (b) Huang, R.-W.; Wei, Y.-S.; Dong, X.-Y.; Wu, X.-H.; Du, C.-
X.; Zang, S.-Q.; Mak, T. C. W. *Nat Chem* **2017**, *9*, 689–697. (c) Xie,

- Y.-P.; Jin, J.-L.; Lu, X.; Mak, T. C. W. *Angew Chem Int Ed* **2015**, *54*,
15176–15180.
15. Scullion, R. A.; Surman, A. J.; Xu, F.; Mathieson, J. S.; Long, D.-L.;
Haso, F.; Liu, T.; Cronin, L. *Angew Chem Int Ed* **2014**, *53*, 10032–
10037.
16. (a) Liu, T. B.; Diemann, E.; Li, H. L.; Dress, A. W. M.; Muller, A.
Nature **2003**, *426*, 59–62. (b) Cardona-Serra, S.; Clemente-Juan, J.
M.; Coronado, E.; Gaita-Ariño, A.; Camón, A.; Evangelisti, M.;
Luis, F.; Martínez-Pérez, M. J.; Sesé, J. *J Am Chem Soc* **2012**, *134*,
14982–14990.
17. (a) Bochtler, M.; Ditzel, L.; Groll, M.; Huber, R. *P Natl Acad Sci*
USA **1997**, *94*, 6070–6074. (b) Ludtke, S. J.; Baker, M. L.; Chen, D.-
H.; Song, J.-L.; Chuang, D. T.; Chiu, W. *Structure* **2008**, *16*, 441–
448.
18. Li, X.-Y.; Tan, Y.-Z.; Yu, K.; Wang, X.-P.; Zhao, Y.-Q.; Sun, D.;
Zheng, L.-S. *Chem-Asian J* **2015**, *10*, 1295–1298.
19. Li, X.-Y.; Wang, Z.; Su, H.-F.; Feng, S.; Kurmoo, M.; Tung, C.-H.;
Sun, D.; Zheng, L.-S. *Nanoscale* *2017*, *9*, 3601–3608.
20. Yam, V. W.-W.; Au, V. K.-M.; Leung, S. Y.-L. *Chem Rev* *2015*,
115, 7589–7728.

TOC

1
2
3
4
5
6
7
8
9
10
11
12
13
14
15
16
17
18
19
20
21
22
23
24
25
26
27
28
29
30
31
32
33
34
35
36
37
38
39
40
41
42
43
44
45
46
47
48
49
50
51
52
53
54
55
56
57
58
59
60

